Loncarevic, A.; Malbasa, Z.; Kovacic, M.; Ostojic, K.; Angaits, A.; Skoko, Z.; Szpunar, J.... (2023). Copper-zinc/chitosan complex hydrogels: Rheological, degradation and biological properties. International Journal of Biological Macromolecules. 251. https://doi.org/10.1016/j.ijbiomac.2023.126373

Copper–zinc/chitosan complex hydrogels: rheological, degradation and biological properties

Andrea Lončarević[1,*], Zoran Malbaša[1], Marin Kovačić[1], Karla Ostojić[2], Ange Angaïts[3], Željko Skoko[4], Joanna Szpunar[3], Inga Urlić[2], Gloria Gallego Ferrer[5,6], Anamarija Rogina[1]

Andrea Lončarević

[1] University of Zagreb, Faculty of Chemical Engineering and Technology, Trg Marka Marulića 19, HR-10000 Zagreb, Croatia

e-mail: aloncarev@fkit.unizg.hr

tel.: +385(0)14597229

* corresponding author

Zoran Malbaša

[1] University of Zagreb, Faculty of Chemical Engineering and Technology, Trg Marka Marulića 19, HR-10000 Zagreb, Croatia

e-mail: zmalbasa@fkit.unizg.hr

Marin Kovačić

[1] University of Zagreb, Faculty of Chemical Engineering and Technology, Trg Marka Marulića 19, HR-10000 Zagreb, Croatia

e-mail: mkovacic@fkit.unizg.hr

Karla Ostojić

[2] University of Zagreb, Faculty of Science, Department of Biology, Horvatovac 102a, HR-10000 Zagreb, Croatia

e-mail: karla.ostojic@biol.pmf.hr

Ange Angaïts

[3] Institute of Analytical and Physical Chemistry for the Environment and Materials (IPREM), University of Pau and the Adour Region, Pau, France

e-mail: ange.angaits@univ-pau.fr

Željko Skoko
[4] University of Zagreb, Faculty of Science, Department of Physics, Bijenička c. 32, HR-10000 Zagreb, Croatia
e-mail: zskoko@phy.hr

Joanna Szpunar
[3] Institute of Analytical and Physical Chemistry for the Environment and Materials (IPREM), University of Pau and the Adour Region, Pau, France
e-mail: joanna.szpunar@univ-pau.fr

Inga Urlić
[2] University of Zagreb, Faculty of Science, Department of Biology, Horvatovac 102a, HR-10000 Zagreb, Croatia
e-mail: ingam@biol.pmf.hr

Gloria Gallego Ferrer
[5] Centre for Biomaterial and Tissue Engineering, Polytechnic University of Valencia, Valencia, Spain
[6] Biomedical Research Networking Center in Bioengineering, Biomaterials and Nanomedicine (CIBER-BBN), Valencia, Spain
e-mail: ggallego@ter.upv.es

Anamarija Rogina
[1] University of Zagreb, Faculty of Chemical Engineering and Technology, Trg Marka Marulića 19, HR-10000 Zagreb, Croatia
e-mail: arogina@fkit.unizg.hr

Graphical abstract

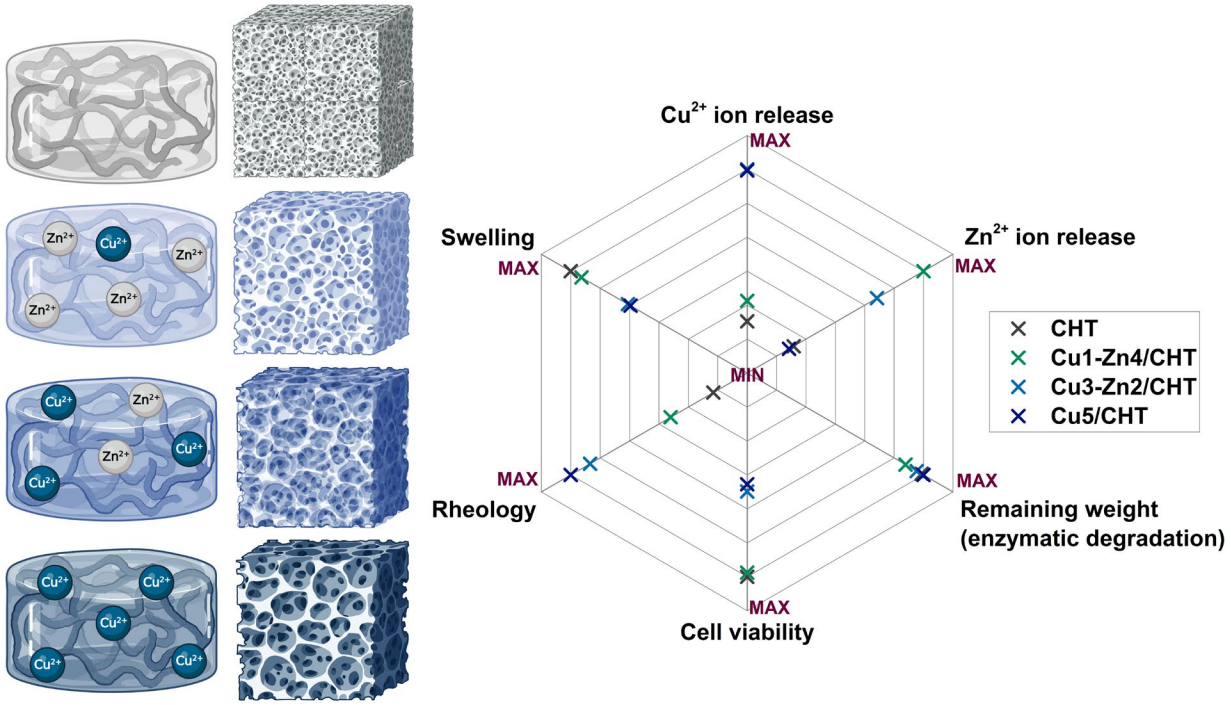

Abstract

The aim of this study was to prepare and investigate the physicochemical and biological properties of bimetallic–chitosan complex hydrogels with different cupric and zinc ions content. Scanning electron microscopy revealed changes in the morphology from the microstructure with larger, tubular pores for aerogels with higher Zn content, to the sheets-like structure with long pores for samples with higher Cu content. The obtained X-ray diffraction patterns showed a broadening of chitosan's characteristic diffraction maximum, decreased swelling ability and increased shear modulus with higher Cu content. ICP-MS results showed that a negligible amount of copper and zinc ions was released during 24 h, implying strong physical crosslink through metal complexation. The accelerated *in vitro* degradation showed good stability during four weeks of lysozyme activity. The MTT assay indicated that the cytotoxicity of Cu^{2+}–Zn^{2+}/chitosan complexes could be adjusted by the amount of cupric ions. All results imply that Cu^{2+} and Zn^{2+} ions act as physical crosslinkers of the polymer network. Also, results are in agreement with the prediction of density functional theory which indicated stronger chitosan–Cu tetrahedral aqua complex interactions in comparison to the chitosan–$[Zn(H_2O)_4)]^{2+}$ interactions.

Keywords: bimetallic–chitosan complex, DFT, SEM, ion release, rheology, cytocompatibility.

1. Introduction

Natural polymer-based materials prepared in the form of scaffolds, microspheres, and fibers have been increasingly investigated for use in bone tissue engineering and regenerative medicine. These materials are mostly based on polysaccharides such as cellulose, starch, alginate, or chitosan (Duceac et al., 2022) and can be used as tissue engineered scaffolds due to the structure and properties similar to glycosaminoglycans which are present in the extracellular matrix (Bahram et al., 2016; Mutlu et al., 2022).

Chitosan has been widely investigated due to its bioactivity, biodegradability, and biocompatibility. It is a linear natural polymer composed of glucosamine and *N*-acetylglucosamine units connected through a β-(1→4) glycosidic bond (Sikorski et al., 2021; Terreux et al., 2006). Its poor mechanical properties are the main limitation of its usage. To overcome that, chitosan is chemically or physically crosslinked (Gritsch et al., 2018). Physical crosslinking can be established through hydrogen bonds, electrostatic and hydrophobic interactions, leading to physical chitosan-based hydrogels with low toxicity (Wang & Zhuang, 2022). On the other hand, the most commonly used chemical crosslinkers are glutaraldehyde (Rohindra et al., 2004), genipin (Dornjak et al., 2022), and epichlorohydrin (Garnica-Palafox et al., 2014). The possibility of harmful and toxic effects of used chemical crosslinkers if not properly removed from chitosan-based hydrogels is another downside (Tang et al., 2020). To overcome these downsides, we propose bimetallic–chitosan complex as an alternative to form strong chitosan-based hydrogels.

Chitosan's ability to form stable chelates with therapeutic metal ions has recently received much attention (Kumar & Koh, 2012). The formation of coordination bonds between metal ions and functional groups of chitosan – amino and hydroxyl groups, could improve the delivery of therapeutic metal ions, consequently improving the biological activity of the polymer (Rogina et al., 2019). It is known that therapeutic ions can be used instead of expensive growth factors and other sensitive biomolecules (Gritsch et al., 2018). Some of the most commonly used metal ions in bone engineering are copper, zinc, and silver (Mouriño et al., 2012). More recently, less abundant metal ions in the human body, such as germanium (Elango et al., 2022), gallium (Akhtar et al., 2021), and vanadium (Cortizo et al., 2016) were also investigated. In this study, the effect of copper (II) and zinc (II) ions' coexistence in the chitosan-based hydrogel was investigated. Cu ions can stimulate biological responses in mesenchymal stem cells, collagen fiber deposition, and blood vessel formation. Also, Cu ions are involved in the regulation of bone metabolism (Kindi et

al., 2021). Prepared Cu^{2+}–alginate hydrogels by Klinkajon and Supaphol (Klinkajon & Supaphol, 2014) also showed great antibacterial activity on positive and negative bacteria, as well as hydrogel's tendency to coagulate fibrin causing the pro-thrombotic coagulation. Like copper ions, zinc ions also inhibit bacteria growth, and wound dressings containing Zn ions are often used for enhanced healing of chronic and acute wounds (Wahid et al., 2018). Furthermore, zinc is involved in bone formation by enhancing osteoblast differentiation, as well as in bone metabolism (Mouriño et al., 2012). However, it is important to emphasize the influence of copper and zinc content in hydrogels, since higher concentrations of these ions may have a cytotoxic effect (Rogina et al., 2019).

Until now, studies on polysaccharide or protein-based materials as a chelating agent were mainly focused on the formation of a monometallic complexes (Gritsch et al., 2018; Mutlu et al., 2022; Rogina et al., 2019; Tang et al., 2020). Recently, bimetallic–polymer complex-based materials were prepared. Shaheen et al. (Shaheen et al., 2021) investigated the mechanical properties, thixotropy, and self-healing ability of a combination of different metal ions (Fe^{3+}, Cu^{2+}, Co^{2+}, Ni^{2+}, and Mn^{2+})–alginate complexes, while Yang et al. (R. Yang et al., 2021) studied the Cu–Zn/gelatin impact on the microstructure reconstruction of the tendon-to-bone insertion and hydrogels' capability of promoting a tenogenesis and osteogenesis. Research groups have shown improved mechanical properties and self-healing ability while decreasing water absorption (Shaheen et al., 2021), and enhanced antibacterial effects and regenerative capacity (R. Yang et al., 2021) when bimetallic–polymer complexes were used. Additionally, the presence of two different metal ions in hydrogel over one metal type might trigger the interactions with different macromolecules (nucleic acids, enzymes) with an impact on a cell metabolism or biological functions (Mouriño et al., 2012). Therefore, the main objective of this study was to prepare and investigate bimetallic–chitosan complex hydrogels with different content of zinc and copper ions. The prepared bimetallic–chitosan hydrogels were investigated in the terms of stability, release of metal ions, rheological properties, and enzymatic degradation under physiological conditions. Also, the microstructure was investigated by scanning electron microscopy, while the cytotoxicity was evaluated by the indirect MTT assay. The results of this research showed that Cu^{2+}–Zn^{2+}/chitosan complex materials with tailored properties could be obtained through facile adjusting of metal content.

2. Experimental part

2.1 Materials

Chitosan (CHT) with a degree of deacetylation (*DD*) 83.2% and viscosity of 293 mPa s (Chitoscience Chitosan 85/200) was purchased from Heppe Medical Chitosan GmbH (Halle (Saale), Germany). Acetic acid (≥ 99.8%) was purchased from Lach-Ner (Neratovice, Czech Republic), and sodium hydroxide (NaOH) from Gram-mol (Zagreb, Croatia). Copper (II) acetate monohydrate (Cu^{2+}) and zinc (II) acetate dehydrate (Zn^{2+}) were purchased from VWR International BDH (Leuven, Belgium).

For the preparation of phosphate-buffered saline solution (PBS, pH 7.4) sodium chloride, potassium chloride, sodium phosphate dibasic, and potassium phosphate monobasic, purchased from Gram-mol (Zagreb, Croatia) were used.

In ICP-MS analysis, Cu and Zn standard solutions (1000 ppm; SCP SCIENCE, Villebon-sur-Yvette, France) were used for the preparation of calibration curves, while Lu was used as an internal standard. Deionized water (18.2 MΩ cm) obtained from a Milli-Q® Direct Q3 Ultrapure Water System (Merck KGaA, Darmstadt, Germany) was used. The dilutions were carried out using a 2% aqueous solution of nitric acid (HNO_3; 70%, Fisher Scientific, Fair Lawn, NJ).

Lysozyme from chicken egg white (~70000 U mg^{-1}; Sigma-Aldrich, St. Louis, USA) and sodium azide (VWR Chemicals BDH, Leuven, Belgium) were used in an enzymatic degradation.

All aqueous solutions were prepared with demineralized water unless otherwise stated. All reagents were of analytical grade and used as received without further purification.

2.2 Preparation of bimetallic–chitosan complex solutions

Firstly, 1 wt.% chitosan solution was prepared by dissolving in 0.5% v/v acetic acid while stirring for 1 h at room temperature. After that, the obtained polymer solution was filtered to remove insoluble parts.

Bimetallic–chitosan complex solutions were prepared with different content of metal ions as stated in Table 1. First, chitosan solution was mixed with Zn^{2+} ions solution while stirring (350 rpm) for 10 minutes at room conditions. After that, the solution of Cu^{2+} ions was added and the bimetallic solution was left for stirring (700 rpm) for 50 min. As a result, a clear transparent Cu^{2+}–Zn^{2+}/chitosan complex solution was obtained. The total amount of Cu^{2+} and Zn^{2+} ions in the bimetallic–chitosan complex solution corresponded to the total molar ratio of

($n(Cu^{2+})+n(Zn^{2+})$):$n(NH_2)$=0.0915:1, while complexes with varying metal content were prepared as follows: $n(Cu^{2+})$:$n(NH_2)$=0.0183:1 and $n(Zn^{2+})$:$n(NH_2)$=0.0732:1 for Cu1–Zn4/CHT system; $n(Cu^{2+})$:$n(NH_2)$=0.0549:1 and $n(Zn^{2+})$:$n(NH_2)$=0.0366:1 for Cu3–Zn2/CHT system, and $n(Cu^{2+})$:$n(NH_2)$=0.0915:1 for Cu5/CHT system.

Table 1. Samples' mark and corresponding weight fraction (w) of Cu^{2+} and Zn^{2+} ions in Cu^{2+}/Zn^{2+}–chitosan complex solutions.

Sample	**CHT**		**Cu1–Zn4/CHT**		**Cu3–Zn2/CHT**		**Cu5/CHT**
$\mathbf{M^{2+}}$	Cu	Zn	Cu1	Zn4	Cu3	Zn2	Cu5
$\boldsymbol{w(M^{2+})}$ **/ %**	0	0	0.62	2.51	1.84	1.27	3.03

2.3 Preparation of bimetallic–chitosan hydrogels

Bimetallic–chitosan hydrogels were prepared by the neutralization of complex solution with 5 wt.% NaOH solution during 24 h. Obtained hydrogels were extensively washed with demineralized water until neutral pH. To maintain the obtained microstructure, Cu^{2+}–Zn^{2+}/CHT hydrogels were frozen and lyophilized.

Chitosan aerogels without metal ion addition served as a control in all measurements. Chitosan aerogels were prepared by lyophilization before neutralization with 5 wt.% NaOH due to insufficient stability of hydrogel obtained according to described procedure. Then, neutralized samples were washed with demineralized water, frozen and lyophilized again.

2.4 Density functional theory (DFT) calculations

Geometry optimizations of the model chitosan molecule (CHT) interacting with Cu or Zn tetrahedral aqua complexes, i.e. $[Cu(H_2O)_4]^{2+}$ and $[Zn(H_2O)_4)]^{2+}$, were performed by utilizing the Gaussian 16 rev. C 01 code (Frisch et al., 2016). GaussView 6 was used for structure preparation, analysis and visualization (Dennington et al., 2016). The PBE0-D3 hybrid functional was chosen due to its good numerical accuracy and implemented dispersion effects (Jaoul et al., 2017; Steinmetz & Grimme, 2013). The 6-31+G(d,p) basis set, a well-proven basis set for the calculations of complexes (Y. Yang et al., 2009), was chosen for H, C, O, and N atoms, whereas the SBKJC-VDZ basis set was chosen for Cu and Zn (Pritchard et al., 2019; Stevens et al., 1992). The optimizations were performed by simulating the solvent effect using the integral equation

196 formalism variant of the polarizable continuum model (IEFPCM). The nature of the minima on
197 the potential energy surface was confirmed to be true minima by numerical frequency calculations.
198 Since $[Cu(H_2O)_4]^{2+}$ is an open-shell system, the stability of the wavefunction of the optimized
199 CHT–$[Cu(H_2O)_4]^{2+}$ complex was confirmed. The counterpoise corrected complexation energies
200 were determined according to the procedure by Riley et al. (Riley et al., 2007). Extended charge
201 decomposition analysis (ECDA) was performed in Multiwfn 3.8 (Gorelsky et al., 2006; T. Lu &
202 Chen, 2012).

203 **2.5 Characterization of bimetallic–chitosan complex materials**

204 ***2.5.1 SEM imaging***

205 Tescan Vega III Easyprobe, (Brno, Czech Republic) with an accelerating voltage of 10 keV was
206 used to investigate the cross-sectional microstructure of bimetallic–chitosan aerogels. Before
207 imaging, samples were sputtered-coated with gold and palladium for 120 s.

208 ***2.5.2 X-ray diffraction analysis***

209 The changes in chitosan crystallinity in the chitosan-based materials were investigated by X-ray
210 diffraction (XRD). X-ray diffraction data were collected at RT on Bruker D8 Discover
211 diffractometer (Bruker AXS GmbH, Karlsruhe, Germany) equipped with LYNXEYE XE-T
212 detector, in Bragg–Brentano geometry. X-ray source was Cu tube with a wavelength of 1.54060
213 Å powered at 1600 W (40 kV and 40 mA) with Ni filter, 2.5° soller slit and fixed slit at 0.4 mm.
214 In the front of a detector, slit opening was 6.5 mm and detector opening was 1.3°. Diffraction peaks
215 were followed from 3° to 70° 2Θ with air scatter at a fixed distance of 0.5 mm from the sample.

216 ***2.5.3 Swelling properties***

217 The swelling capacity of bimetallic–chitosan aerogels was determined by the immersion of
218 samples in a phosphate-buffered saline solution (PBS, pH 7.4) for 24 h at 37 °C. After 24 h, swollen
219 samples were carefully weighed (W_s) and then dried at 40 °C until constant mass (W_d). The
220 swelling capacity was calculated as a difference between wet and dry samples with the respect to
221 the dry weight of the sample: $(W_s\text{-}W_d)/W_d$. Measurements were performed on at least three
222 replicates per system.

2.5.4 Metal ion release

For the determination of released copper and zinc ions content, ~10 mg of bimetallic–chitosan aerogels were incubated in 5 mL of phosphate-buffered saline solution (PBS; pH 7.4) at 37 °C during 24 h. For the measurements of Cu^{2+} and Zn^{2+} ion leaching, obtained supernatants were diluted 25-fold in 2% HNO_3. The analysis was carried out by inductively coupled plasma mass spectrometry (ICP-MS) using a reaction cell pressurized with He and H_2 gas. The isotopes monitored were ^{63}Cu, ^{65}Cu, ^{64}Zn, ^{66}Zn and ^{68}Zn. Analytical blanks were analyzed in parallel. The Standard Reference Material 1643.L1 Trace metals in water (CPAchem Ltd, 2, Bogomilovo, Bulgaria) was used for quality control.

Quantification was performed in the calibration range of 0.1–25 ppb. Measurements were carried out in triplicate, and the results with a relative standard deviation higher than 10% were discarded and the measurements were repeated. Results are reported as mean corrected with a standard deviation of three analytical replicates.

2.5.5 Rheological properties

Rheological properties of bimetallic–chitosan hydrogels (diameter 12 mm, height 1.0–1.5 mm) immersed in PBS (pH 7.4, after 24 h at 37 °C) were determined on Discovery HR-2 Hybrid Rheometer (TA Instruments, New Castle, USA) with a 12 mm parallel Peltier plate and solvent trap cover at 37 °C. The gap between the plane plates was adjusted for each measurement until the axial force was positive (~0.1 N). To prevent the evaporation of water and dehydration of samples during measurements, water drops were applied to the outer edges of the hydrogel sample before testing. The storage and loss moduli of the samples were determined at the frequency range from 0.01 to 10 Hz and constant oscillation strain of 0.1% (previously determined that was within the linear viscoelastic behavior of samples). The measurements were conducted on at least five replicates per system.

2.5.6 Enzymatic degradation

The stability of prepared bimetallic–chitosan aerogels was investigated through *in vitro* enzymatic degradation during four weeks in phosphate-buffered saline solution with lysozyme (1.0 mg mL^{-1}; LZ/PBS) in an orbital shaker (50 rpm) at 37°C. Sodium azide (0.2 mg mL^{-1}) was added as a biocide during the experiment. The medium was refreshed twice a week.

The degradation behavior of chitosan-based aerogels was characterized by weight loss. Initially weighed samples (W_i) were immersed in LZ/PBS solution for a specific time (1, 2, 3, and 4 weeks),

after which were carefully collected, washed three times with demineralized water, and dried at 40 °C until constant mass (W_d). The remaining weight was expressed as (W_d/W_i)×100. Samples incubated in phosphate-buffered saline solution without enzyme (PBS) were used as a control. Measurements were performed in triplicates.

2.5.7 MTT assay

The cytotoxicity of bimetallic–chitosan aerogels was investigated by indirect MTT assay on the human embryonic kidney (HEK293) cell line for 72 h at different concentration of aerogels (1.0, and 0.1 mg mL^{-1}). Before assay, samples were sterilized by UV light for 30 min.

In detail, HEK293 cells were cultured in Dulbecco's modified Eagle medium with 4500 mg L^{-1} glucose (DMEM-high glucose; Capricorn Scientific) supplemented with 10% fetal bovine serum (FBS; Sigma-Aldrich) and 1% penicillin/streptomycin (Sigma-Aldrich). When cells reached 80% confluence, they were seeded in a 96-well plate (Sarsted) in a concentration of 5×10^4 cells/200 µL and allowed to adhere overnight in a humidified incubator with 5% CO_2 at 37 °C. On the same day, samples were immersed in 10 mL of medium and left for 24 hours (5% CO_2, 37 °C).

On the second day, the cell medium was removed and cells were treated with 200 µL of the samples' extract previously centrifuged at 1300 rpm/5 min. Cells were incubated for 24, 48, and 72 hours (5% CO_2, 37 °C).

Following the incubation period, the medium was removed and cells were treated with 40 µL/well of MTT solubilized in cell medium at 0.5 mg mL^{-1} concentration. After 3.5 hours of incubation, 170 µL dimethyl sulfoxide (Sigma-Aldrich) was added to each well to dissolve the formed crystals. After 15 min, absorbance was measured at 560 nm using the microplate reader (Glomax-Multi, Promega). Cell viability was calculated as a percentage of untreated control. Measurements were performed in triplicates.

2.6 Statistical analysis

The results are presented as mean values corrected by standard deviation. Data comparisons were carried out using the two-way analysis of variance (ANOVA) followed by the Tukey *post hoc* test with $p<0.05$ considered as statistically significant. The significant difference between groups is presented as the asterisk (*).

3. Result and discussion

3.1 Computational investigation of interactions between copper and zinc aqua complexes and chitosan

The metal ion–chitosan interactions are still the subject of many researches (Terreux et al., 2006). It is known that the formation of coordination bonds between metal ions and ligands (amino groups on C2 and hydroxyl groups on C3 in the pyranose ring), is determined by the deacetylation degree of chitosan, pH of a solution, and metal ion/chitosan molar ratio (Gritsch et al., 2018; Li et al., 2010; Rhazi et al., 2002). The proposed tetra-coordination models are the "pendant" and "bridge" models. In the "pendant" model, a bivalent metal cation is attached to the amino group and it is coordinated with two hydroxide anions and one hydroxyl group (C3) or water molecule. In the "bridge" model, it is assumed that metal cation coordinates two amino groups from different polymer chains and can form a square-planar structure (Gomes et al., 2014; Rhazi et al., 2002). To investigate these interactions further, we performed density functional theory for interactions between copper and zinc aqua complexes and chitosan in aqueous medium.

Based on the performed computational calculations, the interactions between chitosan and both complexes, $[Cu(H_2O)_4]^{2+}$ and $[Zn(H_2O)_4)]^{2+}$, in aqueous medium are highly favorable. The Cu and Zn metal centers in the aqua complexes form donor type bonds with the amino group in chitosan, resulting in distortion of the tetrahedral aqua complex structure. In the case of the CHT–$[Cu(H_2O)_4]^{2+}$ complex, ECDA determined that a total of 0.78 electrons were donated from chitosan to the copper aqua complex, while for the CHT–$[Zn(H_2O)_4]^{2+}$ complex, a total of 0.24 electrons were donated to the zinc aqua complex. This is reflected in the magnitude of the complexation energies shown in Table 2, where it can be clearly seen that the interactions of chitosan with $[Cu(H_2O)_4]^{2+}$ are stronger than with $[Zn(H_2O)_4]^{2+}$. The interactions of the metal aqua complexes with chitosan provide electrostatic stabilization of CHT in solution, as shown by the electrostatic mapping in Figure 1. The density of the positive charge, i.e. electron affinity, is greater in the case of the CHT–$[Cu(H_2O)_4]^{2+}$ complex and somewhat weaker in the case of the CHT–$[Zn(H_2O)_4]^{2+}$ complex. Thus, the CHT–metal aqua complexes have better solubility in the aqueous medium.

Table 2. Counterpoise corrected complexation energies of chitosan (CHT) and tetrahedral aqua complexes of Cu or Zn, i.e. [Cu(H2O)4]2+ and [Zn(H2O)4)]2+, employing SCRF.

System	Complexation energy / kcal mol^{-1}
CHT–$[Cu(H_2O)_4]^{2+}$	-138.13
CHT–$[Zn(H_2O)_4]^{2+}$	-56.77

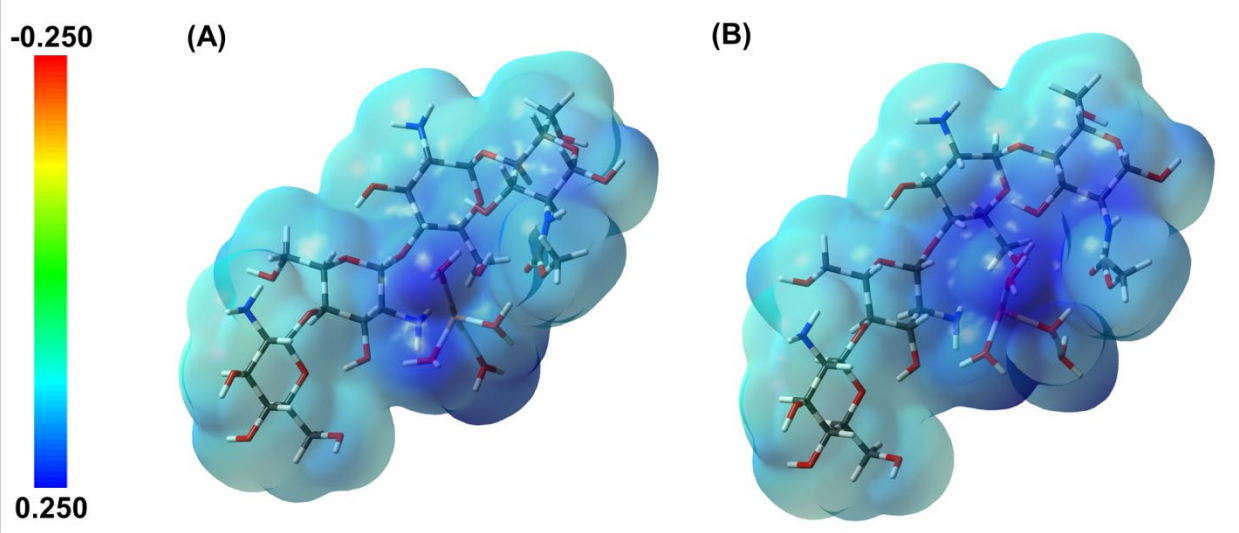

Figure 1. Electrostatic mapping (ESP) of the **(A)** CHT–$[Cu(H_2O)_4]^{2+}$ and **(B)** CHT–$[Zn(H_2O)_4]^{2+}$ complex.

These findings are in agreement with previous results which suggest that copper mainly acts as a bivalent cation and forms a stable (octahedral) structure due to interactions with the nitrogen atoms of amino groups in chitosan (the most favorable site for the coordination) and oxygen atoms in water leading to the stable complex (J. Z. Lu et al., 2008; Terreux et al., 2006). When both metal ions, Cu (II) and Zn (II) ions, are present in the CHT solution, it can be assumed that favorable interaction with the amino group will have cupric ions due to the higher complexation energy of CHT–$[Cu(H_2O)_4]^{2+}$ in regards to the formation of CHT–$[Zn(H_2O)_4]^{2+}$ complexes. Also, due to the formation of stronger interactions polymer–Cu aqua complex, it can be assumed that Cu^{2+} ions will be mainly responsible for stability and improved physicochemical properties of formed bimetallic–chitosan hydrogels.

3.2 Formation of bimetallic–chitosan hydrogels

The formation of physically-crosslinked hydrogels from the chitosan solution can be triggered by the change in environmental conditions like pH or temperature (Bahram et al., 2016). Chitosan is a pH-sensitive polymer that can swell and be dissolved in a slightly acidic aqueous medium (p*K*a 6.2–7.0), while it precipitates in a basic medium. Due to acidic conditions (pH<6), amino groups become protonated which leads to the solubility of polymer. On the contrary, the positive charge on the polymer chains decreases during the neutralization process resulting in polymer precipitation (de Alvarenga, 2011; Tanaka et al., 2014).

In this work, copper–zinc/chitosan complex hydrogels were prepared by *in situ* gelation of complex solution with 5 wt.% sodium hydroxide solution. Following the deprotonation of $–NH_3^+$, physical interactions between metal ions and amino groups in a complex can occur leading to the formation of a stable complex hydrogel (Wahid et al., 2018). All prepared Cu^{2+}–Zn^{2+}/chitosan complex hydrogels kept their stability even after extensive washing with demineralized water. To obtain dry materials and preserve the formed microstructure, bimetallic–chitosan complex hydrogels were frozen and lyophilized. Obtained complex hydrogels and aerogels showed a color change from light blue for the sample with the lowest Cu content (Cu1–Zn4/CHT), to darker blue for Cu5/CHT (Figure 2A). The presence of a color gradient for the Cu1–Zn4/CHT sample was also observed, which could indicate the redistribution of metal ions during the gelation process.

3.3 Microscopic and structural analyses of bimetallic–chitosan aerogels

Scanning electron microscopy (SEM) was used to investigate the cross-sectional morphology of bimetallic–chitosan aerogels, while X-ray diffraction was used to investigate the changes in chitosan crystallinity.

SEM micrographs (Figure 2B-E) confirmed the initial visual assessment indicating different microstructures of bimetallic–chitosan aerogels dependent on the metal ion content. Chitosan aerogel without metal ion addition showed homogeneous, sponge-like morphology with interconnected pores, as previously reported by Zhong et al. (Zhong et al., 2011). The aerogel containing more zinc ions (Cu1–Zn4/CHT) showed larger, tubular pores, while the increase of Cu content changed the microstructure of aerogels to the sheets-like structure with long pores. These results are in accordance with our previous work (Rogina et al., 2019) where monometallic–chitosan aerogels containing Cu^{2+} ions had layered porous structure, while tubular microstructure was observed when Zn^{2+} ions were used as physical crosslinkers. Interestingly, Cu1–Zn4/CHT

aerogel showed a presence of species, possibly metal–based oxide or hydroxide forms, on the inner side of pore walls (Figure 2B, inserted micrograph). These species could be formed due to the neutralization of Cu^{2+}–Zn^{2+}/chitosan complex solution with NaOH solution (Policastro et al., 2022); however, their presence was detected only on a small part of the sample. For biomedical purposes, the presence of pores plays an important role in materials swelling, mechanical properties, controlled degradation kinetics, as well as oxygen, nutrient and waste diffusion for cell growth, adhesion and angiogenesis (Gritsch et al., 2019; Wahid et al., 2018; Zhong et al., 2011). Proposed bimetallic–chitosan aerogels showed controllable microstructure through complexation reactions of Cu^{2+} and Zn^{2+} ions and by varying their amount.

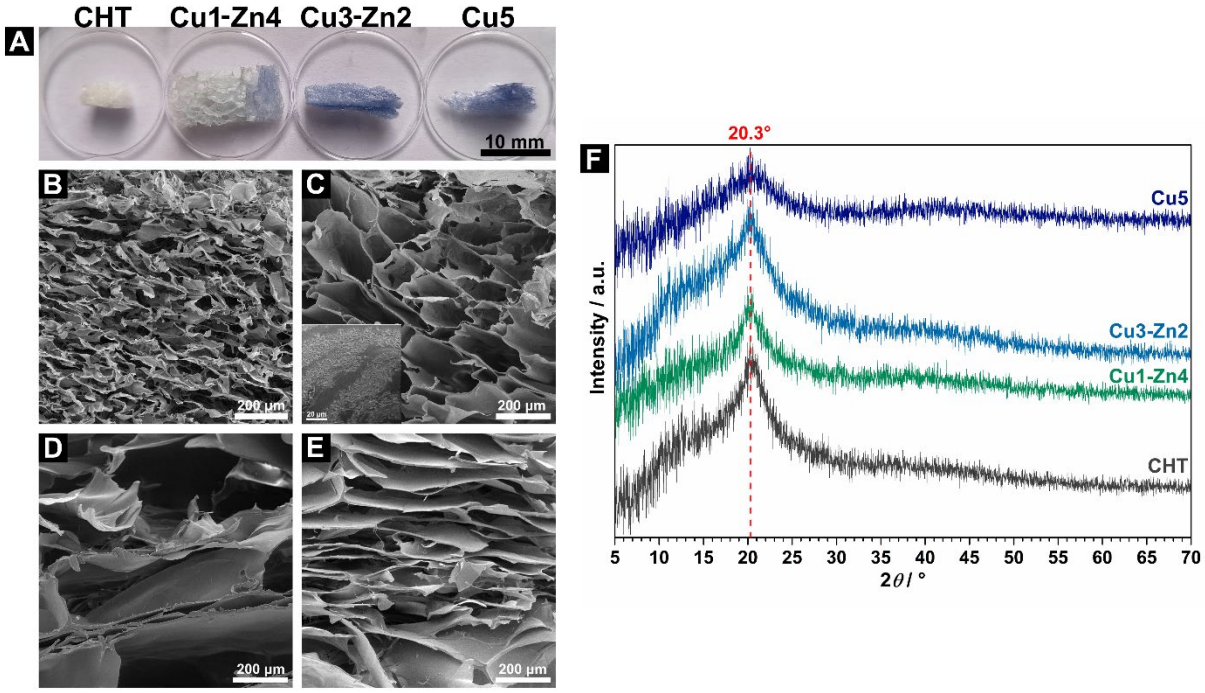

Figure 2. (A) Obtained bimetallic–chitosan complex aerogels. SEM micrographs of cross-sectional morphology of **(B)** chitosan, **(C)** Cu1–Zn4/CHT, **(D)** Cu3–Zn2/CHT, and **(E)** Cu5/CHT bimetallic–chitosan complex aerogels. **(F)** X-ray diffraction patterns of chitosan and bimetallic–chitosan aerogels.

The X-ray diffraction patterns of bimetallic–chitosan aerogels indicated a diffraction maximum at ~20.3° characteristic for semi-crystalline chitosan (Figure 2F). The crystalline structure of the chitosan depends on the number of amino and hydroxyl groups present in the polymer chains. These functional groups can form inter- and intramolecular interactions through hydrogen bonds

which can lead to more ordered structure, i.e. appearing of crystalline regions in the polymer (Khan et al., 2013). The addition of metal ions caused the broadening of the chitosan diffraction maximum, where a wider maximum was observed at higher content of cupric ions. This observation agrees with the literature (Gritsch et al., 2019; Motshekga et al., 2015; Pereira et al., 2017), and it can be described as the reduction of free amino and hydroxyl groups that would be responsible for hydrogen bonds. Since chitosan's functional groups act as ligands for Cu and Zn complexation, the self-assembly of polymer chains through the H-bond is difficult, resulting in decreased crystallinity (Wahid et al., 2017). Additionally, the incorporation of Cu^{2+} and Zn^{2+} ions into the polymer matrix could increase the distance between polymer chains, consequently decreasing inter-chain interactions (Policastro et al., 2022). This effect becomes more noticeable with an increase of Cu^{2+} content in bimetallic–chitosan complex aerogels. These results support our computational prediction of the chitosan–metal ions interactions, which indicated the possibility of stronger interaction between CHT–Cu^{2+} ions than CHT–Zn^{2+} ions. The additional crystalline phase was not detected regardless of the SEM observation, which could suggest its presence at an undetectable amount.

3.4 Physicochemical characterization of bimetallic–chitosan hydrogels

The physicochemical properties in terms of stability (swelling), metal ion leaching, and rheological behavior of prepared bimetallic–chitosan systems were evaluated by immersion of the samples in phosphate-buffered saline solution (PBS, pH 7.4) for 24 hours.

3.4.1 Swelling and rheological properties

Hydrogels are three-dimensional crosslinked macromolecular networks, which can swell in water and biological fluids. This property allows their usage in biomedicine as drug and bioactive molecule carriers and for controlled drug release. The composition and morphology of hydrogels affect their swelling properties (Rohindra et al., 2004). The presence of interconnected pores and thin walls which form an elastic polymer network enables aerogel to absorb a large amount of water (Rufato et al., 2019). In the case of chitosan-based materials, the amino and hydroxyl groups in polymer chains can form hydrogen bonds with water molecules. Besides the degree of deacetylation, the swelling capacity of chitosan depends on the polymer's molecular weight, pH of the incubation medium and crosslink density (Rohindra et al., 2004; Rufato et al., 2019). In this work, the *DD* and pH of the solution were kept the same, so the main influence on the swelling

ability had different content of metal ions and the porosity of bimetallic–chitosan samples. All prepared aerogels possessed a highly porous structure, while visual assessment of hydrogels and aerogels stiffness indicated a more rigid structure at higher Cu content.

Pure chitosan hydrogel showed a swelling ratio of 24.4±1.9 while the addition of a lower amount of Cu (Cu1–Zn4/CHT) slightly decreased the swelling (22.6±1.1), yet without significant difference. Noticeable changes in swelling capacity were detected for samples with higher content of cupric ions (Cu3–Zn2/CHT and Cu5/CHT), which had ~1.6 times lower swelling capacity than Cu1–Zn4/CHT and CHT (Figure 3A). It can be assumed that the swelling ratio of complex hydrogels was decreased due to the introduction of metal ions, which occupied amino and hydroxyl groups and hindered their interactions with water molecules. Also, metal ions serve as (physical) crosslinkers of the polymer chains which makes the hydrogel network less flexible; consequently, the hydrogels have lower swelling capacity (Rohindra et al., 2004). Still, the influence of microstructure and porosity on the absorption ability of aerogels cannot be excluded.

Yang et al. (J. Yang et al., 2019) observed a lower degree of swelling for a non-covalently formed gallic acid modified carboxymethyl chitosan/iron (III) ions hydrogels compared to the hydrogels obtained without Fe^{3+} ions. Similar results were also obtained for chitosan-based hydrogels which were chemically crosslinked with glutaraldehyde (Rohindra et al., 2004). Considering the constant molar ratio of metal ions and amino groups of chitosan in all bimetallic systems, we can assume that cupric ions are mainly responsible for stronger physical crosslinks, which directed the swelling behavior. To support this, we performed a rheological study on bimetallic–chitosan hydrogels.

Hydrogels are viscoelastic soft solids (Wahid et al., 2017), and based on the physical structure of the polymer network, they can be strong (chemically crosslinked polymer gels), weak (colloidal and some biopolymer gels) or pseudo gels (physical entanglements between polymer chains can mimic chemical crosslinks) (Grillet et al., 2012). Moreover, physically crosslinked chitosan-based hydrogels obtained by neutralization have lower shear strength in comparison to the chemically crosslinked hydrogels (Rogina et al., 2017). The neutralization of chitosan solution diminishes charge repulsion from protonated amino groups allowing for network formation through generated intra- and intermolecular interactions, i.e. hydrogen bonding and hydrophobic interactions (Rinaudo, 2006). Here, transition metal ions additionally assisted the formation of stiffer hydrogel through complexation with amino and hydroxyl groups. Similar works (Tang et al., 2020; J. Yang

et al., 2019) on monometallic chitosan-based hydrogels indicated improvement in the rheological properties of hydrogels by metal ion addition.

In this study, the storage (G') and loss (G'') moduli of hydrogels (Figure 3B-D) were determined at frequency of 1 Hz and constant oscillation strain of 0.1% (previously determined by amplitude sweep test, Figure 3D). Figures 3B-C show that storage and loss moduli are significantly higher with the metal ion addition, specifically, higher Cu content resulted in more pronounced moduli increase. Also, samples Cu3–Zn2/CHT and Cu5/CHT have significantly higher G' and G'' values in comparison to the Cu1–Zn4/CHT and control sample (pure CHT). This indicates that metal ions improve stiffness of chitosan-based hydrogels via physical crosslinks, whereas cupric ions had more impact on rheological properties. Furthermore, the loss (damping) factor is the ratio of loss and storage modulus (G''/G') and describes the behavior of crosslinked hydrogels. The material behaves as a viscous liquid if this ratio is higher than 1, while it acts as an elastic solid with a ratio less than 1, i.e. the hydrogel has a greater number of physical networks (Grillet et al., 2012; Wahid et al., 2017). For all bimetallic–chitosan hydrogels, the storage modulus showed higher values compared to the loss modulus indicating the elastic behavior. The amplitude sweep test (Figure 3D) revealed the shortening of the linear viscoelastic region as more Cu^{2+} ions were added. The hydrogel network collapse at lower strains, manifested as the intersection of G' and G'' curves (Sahoo et al., 2022), could imply stiffer network of Cu3–Zn2/CHT and Cu5/CHT with respect to Cu1–Zn4/CHT and CHT hydrogels.

Furthermore, the mechanical properties of hydrogels also rely on their microstructure and swelling properties (Grillet et al., 2012). As shown, with an increase in Cu content, bimetallic–chitosan hydrogels become stiffer and swell less. Otherwise, pure chitosan and Cu1–Zn4/CHT samples showed higher swelling ability but lower G' and G''. The difference in the strength of metal ion physical crosslink between two metals is evident, where copper showed to be more responsible for stronger crosslinking.

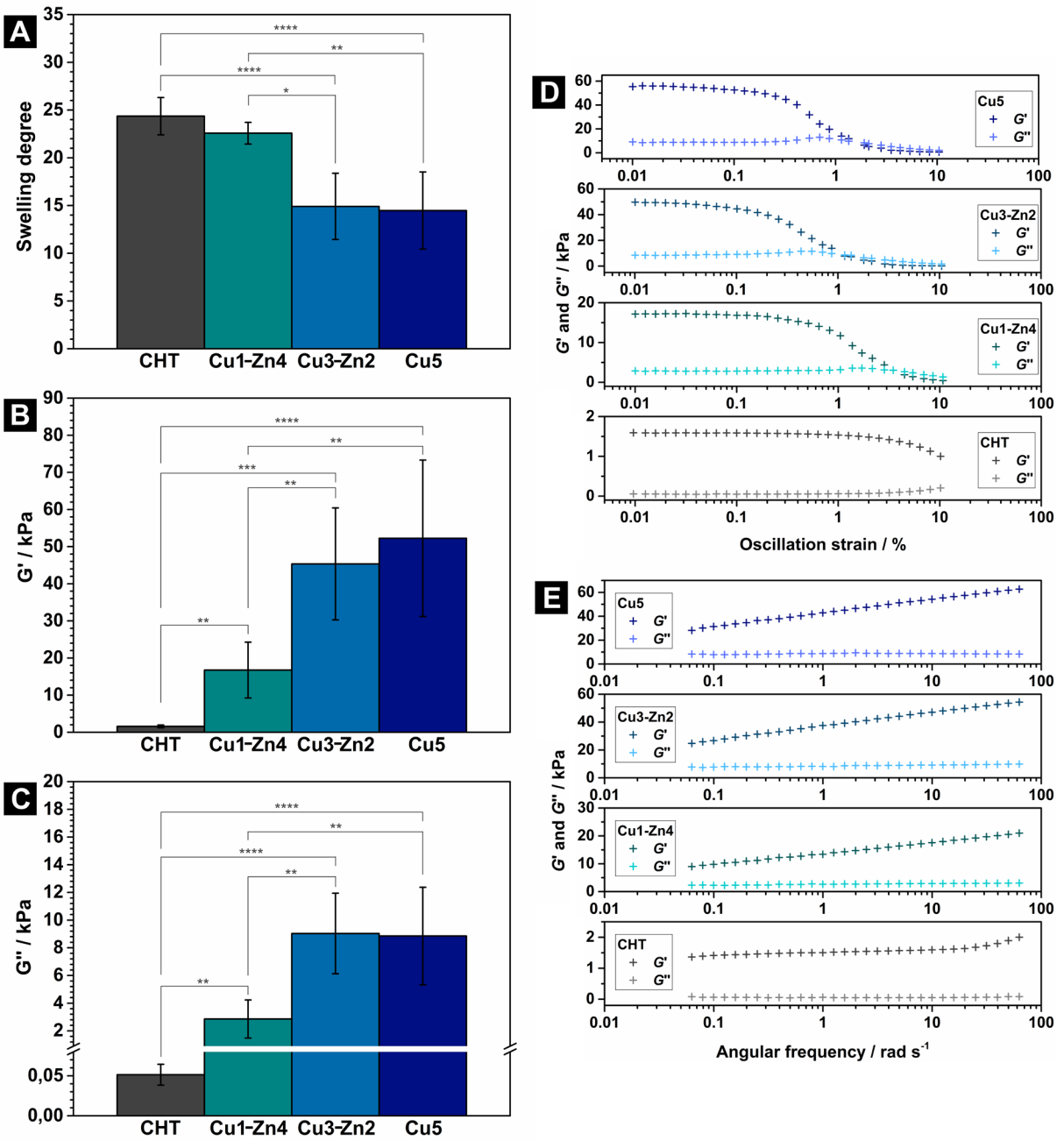
A
Swelling degree
CHT
Cu1-Zn4
Cu3-Zn2
Cu5
B
G' / kPa
C
G'' / kPa
D
G' and G'' / kPa
Oscillation strain / %
E
G' and G'' / kPa
Angular frequency / rad s-1

460

Figure 3. (A) Swelling capacity, **(B)** storage modulus, **(C)** loss modulus, **(D)** strain sweep test, and **(E)** frequency sweep test, after 24-hour immersion of bimetallic–chitosan complex aerogels in phosphate-buffered saline solution, pH 7.4, 37 °C. The *G′* and *G″* curves represent the average values of min. five replicates. The error bars were excluded for the sake of clarity. Significant difference between groups: * $p<0.05$, ** $p<0.01$, *** $p<0.001$, and **** $p<0.0001$.

3.4.2 Cu^{2+} and Zn^{2+} ion release

The quantities of released Cu^{2+} and Zn^{2+} ions in samples' supernatants were measured by ICP-MS. It was shown (Figure 4) that a negligible amount of Cu (II) and Zn (II) ions is released during 24 h which indicated good stability of prepared bimetallic–chitosan hydrogels. The maximum metal ion leaching is reached within first six hours for all bimetallic–chitosan hydrogels, pointing out a burst effect during the first hour. Then, a slight decrease in ion concentration was detected after 24 h, which could indicate possible salt precipitation. According to Mutlu et al. (Mutlu et al., 2022), it is possible that zinc forms water-insoluble phosphate compounds, decreasing the concentration of metal ions in the supernatant. This could result in high standard deviations as seen for Zn^{2+} ion release during first six hours. A similar observation is noticed for chitosan–Zn complex-based films in Tris/HCl buffer solution (pH 7.4) (Mutlu et al., 2022), which was explained as initial Zn^{2+} ions leaching from the surface layer and further slower release due to longer diffusion paths.

Furthermore, a larger amount of released Zn^{2+} ions was expected due to the weaker complexation. Indeed, sample Cu3–Zn2/CHT showed a higher leaching effect of Zn^{2+} ions than cupric ions. Quick release of cupric ions was also reported on similar chitosan-Cu (II) complex hydrogels (Gritsch et al., 2019), with no significant changes in released quantity during 21 days of incubation. The authors concluded that a significant amount of copper is remained in hydrogel and will be released only in the presence of an enzyme.

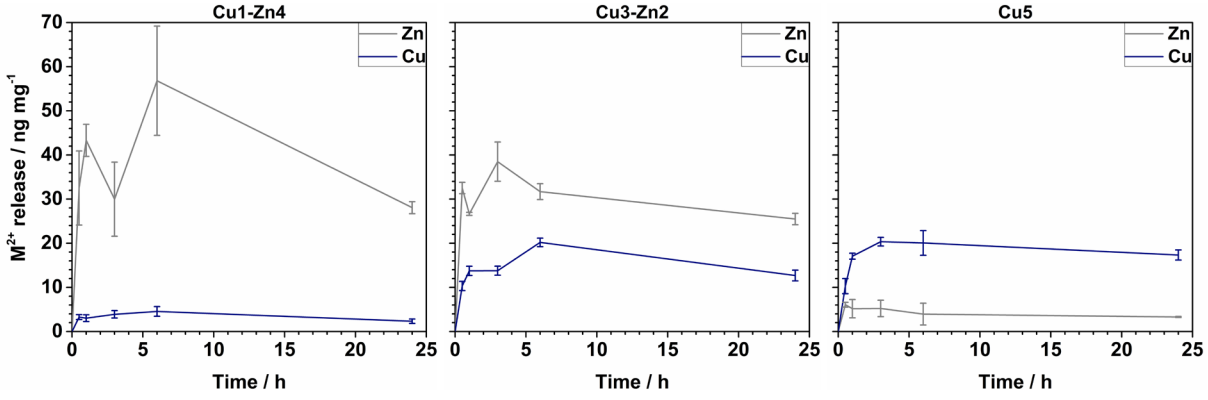

Figure 4. Cu and Zn ion release from bimetallic–chitosan complex aerogels incubated in phosphate-buffered saline solution (PBS, pH 7.4) at 37 °C during 24 h.

3.5 Enzymatic degradation

The *in vitro* enzymatic degradation was performed to investigate the stability of bimetallic–chitosan hydrogels during longer incubation period. The degradation of hydrogels was investigated in phosphate-buffered saline solution with lysozyme (LZ/PBS), while hydrogels incubated in PBS without lysozyme (PBS) were used as a control.

The gravimetric analysis showed that the stability of the prepared chitosan-based samples remains constant during incubation time (Figure 5). After 4 weeks in LZ/PBS medium, the most stable was Cu5/CHT hydrogel with weight loss of ~5%, while Cu1–Zn4/CHT sample had the highest weight loss (~16%). As expected, the weight loss increases for all samples during incubation time in LZ/PBS medium. Lysozyme hydrolyses specific linkage between two *N*-acetylglucosamine units in polysaccharides (Solomons et al., 2016). Considering that chitosan with a *DD* of 83.2% was used, the number of possible glycosidic bonds on which lysozyme acts is limited. The biodegradability of chitosan-based hydrogels is an important parameter for its biomedical application. In bone tissue engineering it is important to obtain material that is able to degrade at the same rate as the formation of new tissue (Ressler, 2022). It can be concluded that bimetallic–chitosan hydrogels are resistant to enzyme activity even at extremely high concentration and stable under physiological pH for longer incubation time.

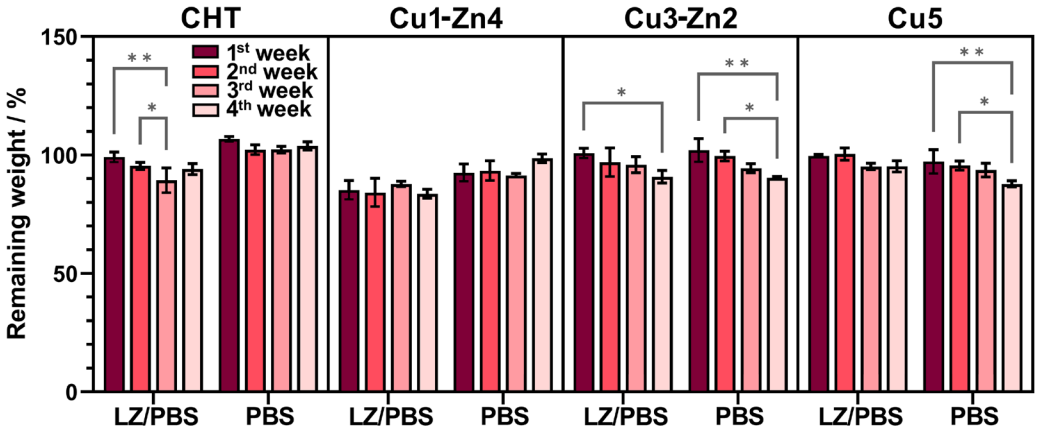

Figure 5. *In vitro* degradation of bimetallic–chitosan hydrogels in phosphate-buffered saline solution with and without lysozyme activity. Significant difference between groups: * $p<0.05$, ** $p<0.01$, *** $p<0.001$, and **** $p<0.0001$.

3.6 Indirect *in vitro* cytotoxicity study

The results of the cytotoxicity assay are shown in Figure 6. Cu3–Zn2/CHT and Cu5/CHT hydrogels showed cytotoxic activity at higher concentration (1.0 mg mL^{-1}) after 48 h of incubation. On the contrary, Cu1–Zn4/CHT hydrogel supported good cell viability at the same materials concentration. At lower materials concentration, all prepared bimetallic–chitosan systems indicated non-cytotoxicity after 72 h of incubation, while Cu1–Zn4/CHT even supported cell proliferation. Copper and zinc ions are considered as therapeutic metal ions, that have important roles in bone regeneration (Kindi et al., 2021). Besides the anti-inflammatory and antibiotic properties, copper and zinc ions have stimulative effects on osteogenesis and angiogenesis, which consequently improve bone formation (Hoppe et al., 2013). As already reported (Gritsch et al., 2019), copper in concentrations higher than 30 ppm has a cytotoxic effect. According to our ICP-MS results, it was expected that the bimetallic–chitosan samples are non-cytotoxic. Surprisingly, the cell viability assay indicated a cytotoxic effect even at negligible concentration of ions detected in release experiment. Furthermore, Gritsch et al. (Gritsch et al., 2019) reported on the correlation between released copper ions from chitosan-copper (II) complex and the viability of MG-63 cells cultured in direct contact with material. A possible explanation for this discrepancy is the interactions of copper and zinc with components of the culture medium. It is assumed that metal ions interact with amino-rich components (proteins) in the incubation medium through the formation of coordinative bonds (Kindi et al., 2021). There might be a significant release of Cu^{2+} ions from bimetallic–chitosan complex material in the cell culture medium with respect to the buffer solution, as evident from low cell viability. From this perspective, it is paramount to investigate the behavior of metal-containing hydrogels in a protein-supplemented medium, which will be a focus of future research.

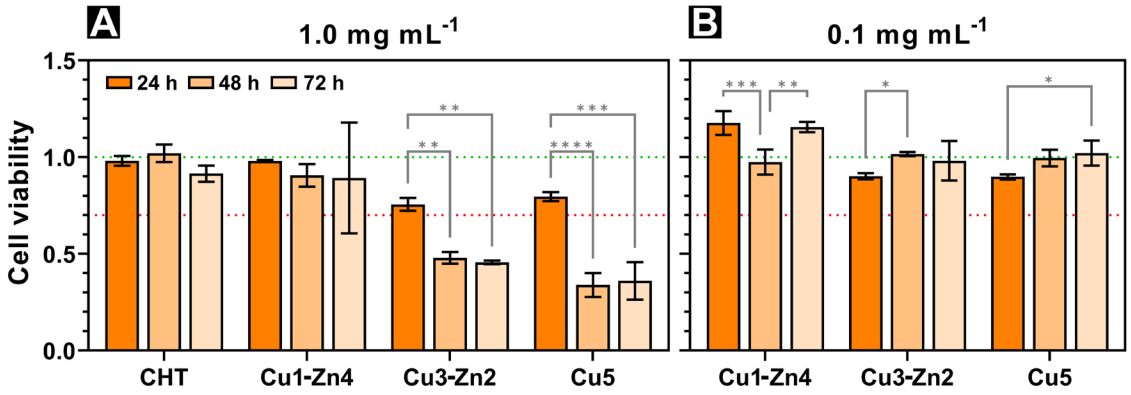

Figure 6. MTT assay on HEK293 cells incubated with materials supernatant material concentration of **(A)** 1.0 mg mL^{-1}, and **(B)** 0.1 mg mL^{-1}, during 24, 48 and 72 h of incubation. Significant difference between groups: * $p<0.05$, ** $p<0.01$, *** $p<0.001$, and **** $p<0.0001$.

4. Conclusions

Chitosan possesses good biodegradability and biocompatibility; however, its poor mechanical properties can limit biomedical applications. To overcome this limitation, chitosan's ability to form stable chelates with metal ions, such as copper and zinc, is used to prepare strong physically crosslinked hydrogels. In this work, bimetallic–chitosan complex hydrogels were prepared by *in situ* gelation. Density functional theory indicated stronger interactions between chitosan's amino groups with $[Cu(H_2O)_4]^{2+}$ than $[Zn(H_2O)_4]^{2+}$ in an aqueous medium. The morphology of bimetallic–chitosan hydrogels was dependent on Cu content. Samples with lower Cu content had larger, tubular pores, while the higher Cu content changed the microstructure to a sheet-like structure with long pores. X-ray diffraction patterns of bimetallic–chitosan samples indicated changes in chitosan crystallinity with the introduction of copper and zinc ions. The swelling ability of bimetallic-chitosan aerogels was lower with the increase of Cu content, while storage and loss moduli were improved. The results indicated that metal ions served as physical crosslinkers of the polymer which makes the hydrogel network stiffer. All prepared hydrogels showed good stability during four weeks of enzymatic degradation. Finally, bimetallic–chitosan hydrogels' cytocompatibility can be modulated by the quantity of copper (II) ions giving more possibilities for biomedical applications.

Acknowledgment

This work was supported by the Croatian Science Foundation [grant number UIP-2020-02-6201]. A.L. acknowledges Biorender.com. Ž.S. acknowledges CeNIKS project financed from the European Regional Development Fund, OP "Competitiveness and Cohesion" 2014-2020. M.K. and A.R. acknowledge Isabella computational cluster. G.G.F. acknowledges grant number PID2019-106000RB-C21 funded by MCIN/AEI/10.13039/501100011033.

CRediT roles: A. Lončarević, Z. Malbaša, A. Rogina: Conceptualization; A. Lončarević, Z. Malbaša: Data curation; A. Lončarević, Z. Malbaša, G. Gallego Ferrer: Formal analysis; A. Rogina: Funding acquisition; A. Lončarević, Z. Malbaša, K. Ostojić, A. Angaïts, M. Kovačić, Ž. Skoko, G. Gallego Ferrer: Investigation; G. Gallego Ferrer, I. Urlić, A. Rogina: Methodology; A. Rogina: Project administration; J. Szpunar, Ž. Skoko, G. Gallego Ferrer, I. Urlić, A. Rogina: Resources; G. Gallego Ferrer, J. Szpunar, I. Urlić, A. Rogina: Supervision; A. Lončarević, Z. Malbaša: Writing - original draft; M. Kovačić, G. Gallego Ferrer, A. Rogina: Writing - review & editing.

References

Akhtar, M. A., Hadzhieva, Z., Ilyas, K., Ali, M. S., Peukert, W., & Boccaccini, A. R. (2021). Facile Synthesis of Gallium (III)-Chitosan Complexes as Antibacterial Biomaterial. *Pharmaceutics*, *13*, 1702. https://doi.org/10.3390/pharmaceutics13101702

Bahram, M., Mohseni, N., & Moghtader, M. (2016). An Introduction to Hydrogels and Some Recent Applications. In S. B. Majee (Ed.), *Emerging Concepts in Analysis and Applications of Hydrogels* (pp. 9–38). InTech. https://doi.org/10.5772/64301

Cortizo, A. M., Ruderman, G., Mazzini, F. N., Molinuevo, M. S., & Mogilner, I. G. (2016). Novel Vanadium-Loaded Ordered Collagen Scaffold Promotes Osteochondral Differentiation of Bone Marrow Progenitor Cells. *International Journal of Biomaterials*, *2016*, 1–11. https://doi.org/10.1155/2016/1486350

de Alvarenga, E. S. (2011). Characterization and Properties of Chitosan Elson. In M. Elnashar (Ed.), *Biotechnology of Biopolymers* (pp. 91–108). InTech. https://doi.org/10.5772/17020

Dennington, R., Keith, T. A., & Millam, J. M. (2016). *Gaussview Version 6, Semichem Inc. Shawnee Mission KS*.

Dornjak, L., Kovačić, M., Ostojić, K., Angaits, A., Szpunar, J., Urlić, I., & Rogina, A. (2022).

583 Chitosan-Boric Acid Scaffolds for Doxorubicin Delivery in the Osteosarcoma Treatment.
584 *Polymers*, *14*(21), 4753. https://doi.org/10.3390/polym14214753
585 Duceac, I. A., Stanciu, M.-C., Nechifor, M., Tanasă, F., & Teacă, C.-A. (2022). Insights on Some
586 Polysaccharide Gel Type Materials and Their Structural Peculiarities. *Gels*, *8*(12), 771.
587 https://doi.org/10.3390/gels8120771
588 Elango, J., Bushin, R., Lijnev, A., De Aza, P. N., Martínez, C. P.-A., Marín, J. M. G., Hernandez,
589 A. B., Olmo, L. R. M., & Val, J. E. M. S. De. (2022). The Effect of Germanium-Loaded
590 Hydroxyapatite Biomaterials on Bone Marrow Mesenchymal Stem Cells Growth. *Cells*,
591 *11*(19), 2993. https://doi.org/10.3390/cells11192993
592 Frisch, M. J., Trucks, G. W., Schlegel, H. B., Scuseria, G. E., Robb, M. a., Cheeseman, J. R.,
593 Scalmani, G., Barone, V., Petersson, G. a., Nakatsuji, H., Li, X., Caricato, M., Marenich, a.
594 V., Bloino, J., Janesko, B. G., Gomperts, R., Mennucci, B., Hratchian, H. P., Ortiz, J. V., …
595 Fox, D. J. (2016). *G16_C01* (p. Gaussian 16, Revision A.03, Gaussian, Inc., Wallin).
596 Garnica-Palafox, I. M., Sánchez-Arévalo, F. M., Velasquillo, C., García-Carvajal, Z. Y., García-
597 López, J., Ortega-Sánchez, C., Ibarra, C., Luna-Bárcenas, G., & Solís-Arrieta, L. (2014).
598 Mechanical and structural response of a hybrid hydrogel based on chitosan and poly(vinyl
599 alcohol) cross-linked with epichlorohydrin for potential use in tissue engineering. *Journal of*
600 *Biomaterials Science, Polymer Edition*, *25*(1), 32–50.
601 https://doi.org/10.1080/09205063.2013.833441
602 Gomes, J. R. B., Jorge, M., & Gomes, P. (2014). Interaction of chitosan and chitin with Ni, Cu and
603 Zn ions: A computational study. *The Journal of Chemical Thermodynamics*, *73*, 121–129.
604 https://doi.org/10.1016/j.jct.2013.11.016
605 Gorelsky, S. I., Ghosh, S., & Solomon, E. I. (2006). Mechanism of N2O Reduction by the μ4-S
606 Tetranuclear CuZ Cluster of Nitrous Oxide Reductase. *Journal of the American Chemical*
607 *Society*, *128*(1), 278–290. https://doi.org/10.1021/ja055856o
608 Grillet, A. M., Wyatt, N. B., & Gloe, L. M. (2012). Polymer Gel Rheology and Adhesion. In J. De
609 Vicente (Ed.), *Rheology* (Issue 3, pp. 59–80). InTech. https://doi.org/10.5772/36975
610 Gritsch, L., Lovell, C., Goldmann, W. H., & Boccaccini, A. R. (2018). Fabrication and
611 characterization of copper(II)-chitosan complexes as antibiotic-free antibacterial biomaterial.
612 *Carbohydrate Polymers*, *179*, 370–378. https://doi.org/10.1016/j.carbpol.2017.09.095
613 Gritsch, L., Maqbool, M., Mouriño, V., Ciraldo, F. E., Cresswell, M., Jackson, P. R., Lovell, C.,

& Boccaccini, A. R. (2019). Chitosan/hydroxyapatite composite bone tissue engineering scaffolds with dual and decoupled therapeutic ion delivery: copper and strontium. *Journal of Materials Chemistry B*, *7*, 6109–6124. https://doi.org/10.1039/C9TB00897G

Hoppe, A., Mouriño, V., & Boccaccini, A. R. (2013). Therapeutic inorganic ions in bioactive glasses to enhance bone formation and beyond. *Biomater. Sci.*, *1*(3), 254–256. https://doi.org/10.1039/C2BM00116K

Jaoul, A., Nocton, G., & Clavaguéra, C. (2017). Assessment of Density Functionals for Computing Thermodynamic Properties of Lanthanide Complexes. *ChemPhysChem*, *18*(19), 2688–2696. https://doi.org/10.1002/cphc.201700629

Khan, A., Mehmood, S., Shafiq, M., Yasin, T., Akhter, Z., & Ahmad, S. (2013). Structural and antimicrobial properties of irradiated chitosan and its complexes with zinc. *Radiation Physics and Chemistry*, *91*, 138–142. https://doi.org/10.1016/j.radphyschem.2013.05.025

Kindi, H., Menzel, M., Heilmann, A., Schmelzer, C. E. H., Herzberg, M., Fuhrmann, B., Gallego-Ferrer, G., & Groth, T. (2021). Effect of metal ions on the physical properties of multilayers from hyaluronan and chitosan, and the adhesion, growth and adipogenic differentiation of multipotent mouse fibroblasts. *Soft Matter*, *17*(36), 8394–8410. https://doi.org/10.1039/D1SM00405K

Klinkajon, W., & Supaphol, P. (2014). Novel copper (II) alginate hydrogels and their potential for use as anti-bacterial wound dressings. *Biomedical Materials*, *9*(4), 045008. https://doi.org/10.1088/1748-6041/9/4/045008

Kumar, S., & Koh, J. (2012). Physiochemical, Optical and Biological Activity of Chitosan-Chromone Derivative for Biomedical Applications. *International Journal of Molecular Sciences*, *13*(5), 6102–6116. https://doi.org/10.3390/ijms13056102

Li, S.-D., Zhang, C.-H., Dong, J.-J., Ou, C.-Y., Quan, W.-Y., Yang, L., & She, X.-D. (2010). Effect of cupric ion on thermal degradation of quaternized chitosan. *Carbohydrate Polymers*, *81*(2), 182–187. https://doi.org/10.1016/j.carbpol.2010.02.049

Lu, J. Z., Duan, X., Wu, Q., & Lian, K. (2008). Chelating efficiency and thermal, mechanical and decay resistance performances of chitosan copper complex in wood–polymer composites. *Bioresource Technology*, *99*(13), 5906–5914. https://doi.org/10.1016/j.biortech.2007.09.086

Lu, T., & Chen, F. (2012). Multiwfn: A multifunctional wavefunction analyzer. *Journal of Computational Chemistry*, *33*(5), 580–592. https://doi.org/10.1002/jcc.22885

Motshekga, S. C., Ray, S. S., Onyango, M. S., & Momba, M. N. B. (2015). Preparation and antibacterial activity of chitosan-based nanocomposites containing bentonite-supported silver and zinc oxide nanoparticles for water disinfection. *Applied Clay Science*, *114*, 330–339. https://doi.org/10.1016/j.clay.2015.06.010

Mouriño, V., Cattalini, J. P., & Boccaccini, A. R. (2012). Metallic ions as therapeutic agents in tissue engineering scaffolds: an overview of their biological applications and strategies for new developments. *Journal of The Royal Society Interface*, *9*(68), 401–419. https://doi.org/10.1098/rsif.2011.0611

Mutlu, N., Liverani, L., Kurtuldu, F., Galusek, D., & Boccaccini, A. R. (2022). Zinc improves antibacterial, anti-inflammatory and cell motility activity of chitosan for wound healing applications. *International Journal of Biological Macromolecules*, *213*(May), 845–857. https://doi.org/10.1016/j.ijbiomac.2022.05.199

Pereira, F. S., Lanfredi, S., González, E. R. P., da Silva Agostini, D. L., Gomes, H. M., & dos Santos Medeiros, R. (2017). Thermal and morphological study of chitosan metal complexes. *Journal of Thermal Analysis and Calorimetry*, *129*(1), 291–301. https://doi.org/10.1007/s10973-017-6146-2

Policastro, D., Giorno, E., Scarpelli, F., Godbert, N., Ricciardi, L., Crispini, A., Candreva, A., Marchetti, F., Xhafa, S., De Rose, R., Nucera, A., Barberi, R. C., Castriota, M., De Bartolo, L., & Aiello, I. (2022). New Zinc-Based Active Chitosan Films: Physicochemical Characterization, Antioxidant, and Antimicrobial Properties. *Frontiers in Chemistry*, *10*(May), 1–16. https://doi.org/10.3389/fchem.2022.884059

Pritchard, B. P., Altarawy, D., Didier, B., Gibson, T. D., & Windus, T. L. (2019). New Basis Set Exchange: An Open, Up-to-Date Resource for the Molecular Sciences Community. *Journal of Chemical Information and Modeling*, *59*(11), 4814–4820. https://doi.org/10.1021/acs.jcim.9b00725

Ressler, A. (2022). Chitosan-Based Biomaterials for Bone Tissue Engineering Applications: A Short Review. *Polymers*, *14*(16), 3430. https://doi.org/10.3390/polym14163430

Rhazi, M., Desbrières, J., Tolaimate, A., Rinaudo, M., Vottero, P., & Alagui, A. (2002). Contribution to the study of the complexation of copper by chitosan and oligomers. *Polymer*, *43*(4), 1267–1276. https://doi.org/10.1016/S0032-3861(01)00685-1

Riley, K. E., Vondrášek, J., & Hobza, P. (2007). Performance of the DFT-D method, paired with

the PCM implicit solvation model, for the computation of interaction energies of solvated complexes of biological interest. *Physical Chemistry Chemical Physics*, *9*(41), 5555–5560. https://doi.org/10.1039/b708089a

Rinaudo, M. (2006). Non-Covalent Interactions in Polysaccharide Systems. *Macromolecular Bioscience*, *6*(8), 590–610. https://doi.org/10.1002/mabi.200600053

Rogina, A., Lončarević, A., Antunović, M., Marijanović, I., Ivanković, M., & Ivanković, H. (2019). Tuning physicochemical and biological properties of chitosan through complexation with transition metal ions. *International Journal of Biological Macromolecules*, *129*, 645–652. https://doi.org/10.1016/j.ijbiomac.2019.02.075

Rogina, A., Ressler, A., Matić, I., Gallego Ferrer, G., Marijanović, I., Ivanković, M., & Ivanković, H. (2017). Cellular hydrogels based on pH-responsive chitosan-hydroxyapatite system. *Carbohydrate Polymers*, *166*, 173–182. https://doi.org/10.1016/j.carbpol.2017.02.105

Rohindra, D. R., Nand, A. V, & Khurma, J. R. (2004). Swelling properties of chitosan hydrogels. *The South Pacific Journal of Natural and Applied Sciences*, *22*(1), 32–35. https://doi.org/10.1071/SP04005

Rufato, K. B., Galdino, J. P., Ody, K. S., Pereira, A. G. B., Corradini, E., Martins, A. F., Paulino, A. T., Fajardo, A. R., Aouada, F. A., La Porta, F. A., Rubira, A. F., & Muniz, E. C. (2019). Hydrogels Based on Chitosan and Chitosan Derivatives for Biomedical Applications. In L. Popa, M. V. Ghica, & C. Dinu-Pirvu (Eds.), *Hydrogels - Smart Materials for Biomedical Applications* (pp. 59–98). IntechOpen. https://doi.org/10.5772/intechopen.78482

Sahoo, S. D., Vasudha, T. K., Muthuvijayan, V., & Prasad, E. (2022). Chitosan-Based Self-Healable and Adhesive Hydrogels for Flexible Strain Sensor Application. *ACS Applied Polymer Materials*, *4*(12), 9176–9185. https://doi.org/10.1021/acsapm.2c01488

Shaheen, A., Maswal, M., & Dar, A. A. (2021). Synergistic effect of various metal ions on the mechanical, thixotropic, self-healing, swelling and water retention properties of bimetallic hydrogels of alginate. *Colloids and Surfaces A: Physicochemical and Engineering Aspects*, *627*(July), 127223. https://doi.org/10.1016/j.colsurfa.2021.127223

Sikorski, D., Gzyra-Jagieła, K., & Draczyński, Z. (2021). The Kinetics of Chitosan Degradation in Organic Acid Solutions. *Marine Drugs*, *19*(5), 236. https://doi.org/10.3390/md19050236

Solomons, G. T. W., Fryhle, C. B., & Snyder, S. A. (2016). *Organic Chemistry* (12th ed.). John Wiley & Sons, Inc.

Steinmetz, M., & Grimme, S. (2013). Benchmark Study of the Performance of Density Functional Theory for Bond Activations with (Ni,Pd)-Based Transition-Metal Catalysts. *ChemistryOpen*, *2*(3), 115–124. https://doi.org/10.1002/open.201300012

Stevens, W. J., Krauss, M., Basch, H., & Jasien, Paul, G. (1992). Relativistic compact effective potentials and efficient, shared-exponent basis sets for the third-, fourth-, and fifth-row atoms. *Canadian Journal of Chemistry*, *70*, 612–630. https://doi.org/10.1139/v92-085

Tanaka, K., Nishida, K., Gabrys, B. J., Lawrence, M. J., & Kanaya, T. (2014). Critical dissolution ionic strength of aqueous solution of chitosan hydrochloride salt. *Journal of Fiber Science and Technology*, *70*(9), 225–231. https://doi.org/10.2115/fiber.70.225

Tang, S., Yang, J., Lin, L., Peng, K., Chen, Y., Jin, S., & Yao, W. (2020). Construction of physically crosslinked chitosan/sodium alginate/calcium ion double-network hydrogel and its application to heavy metal ions removal. *Chemical Engineering Journal*, *393*(January), 124728. https://doi.org/10.1016/j.cej.2020.124728

Terreux, R., Domard, M., Viton, C., & Domard, A. (2006). Interactions Study between the Copper II Ion and Constitutive Elements of Chitosan Structure by DFT Calculation. *Biomacromolecules*, *7*(1), 31–37. https://doi.org/10.1021/bm0504126

Wahid, F., Wang, H.-S., Zhong, C., & Chu, L.-Q. (2017). Facile fabrication of moldable antibacterial carboxymethyl chitosan supramolecular hydrogels cross-linked by metal ions complexation. *Carbohydrate Polymers*, *165*, 455–461. https://doi.org/10.1016/j.carbpol.2017.02.085

Wahid, F., Zhou, Y.-N., Wang, H.-S., Wan, T., Zhong, C., & Chu, L.-Q. (2018). Injectable self-healing carboxymethyl chitosan-zinc supramolecular hydrogels and their antibacterial activity. *International Journal of Biological Macromolecules*, *114*(2017), 1233–1239. https://doi.org/10.1016/j.ijbiomac.2018.04.025

Wang, J., & Zhuang, S. (2022). Chitosan-based materials: Preparation, modification and application. *Journal of Cleaner Production*, *355*(January), 131825. https://doi.org/10.1016/j.jclepro.2022.131825

Yang, J., Li, M., Wang, Y., Wu, H., Ji, N., Dai, L., Li, Y., Xiong, L., Shi, R., & Sun, Q. (2019). High-Strength Physically Multi-Cross-Linked Chitosan Hydrogels and Aerogels for Removing Heavy-Metal Ions. *Journal of Agricultural and Food Chemistry*, *67*(49), 13648–13657. https://doi.org/10.1021/acs.jafc.9b05063

738 Yang, R., Li, G., Zhuang, C., Yu, P., Ye, T., Zhang, Y., Shang, P., Huang, J., Cai, M., Wang, L.,
739 Cui, W., & Deng, L. (2021). Gradient bimetallic ion–based hydrogels for tissue
740 microstructure reconstruction of tendon-to-bone insertion. *Science Advances*, *7*(26), 1–14.
741 https://doi.org/10.1126/sciadv.abg3816
742 Yang, Y., Weaver, M. N., & Merz, K. M. (2009). Assessment of the "6-31+G** + LANL2DZ"
743 Mixed Basis Set Coupled with Density Functional Theory Methods and the Effective Core
744 Potential: Prediction of Heats of Formation and Ionization Potentials for First-Row-
745 Transition-Metal Complexes. *The Journal of Physical Chemistry A*, *113*(36), 9843–9851.
746 https://doi.org/10.1021/jp807643p
747 Zhong, X., Ji, C., Chan, A. K. L., Kazarian, S. G., Ruys, A., & Dehghani, F. (2011). Fabrication
748 of chitosan/poly(ε-caprolactone) composite hydrogels for tissue engineering applications.
749 *Journal of Materials Science: Materials in Medicine*, *22*(2), 279–288.
750 https://doi.org/10.1007/s10856-010-4194-2
751